

# Electrocatalytic Oxidation of Alcohol with Cobalt Triphosphine Complexes

Spencer P. Heins, Patrick E. Schneider, Amy L. Speelman, Sharon Hammes-Schiffer,\* and Aaron M. Appel\*

Cite This: *ACS Catal.* 2021, 11, 6384–6389

Read Online

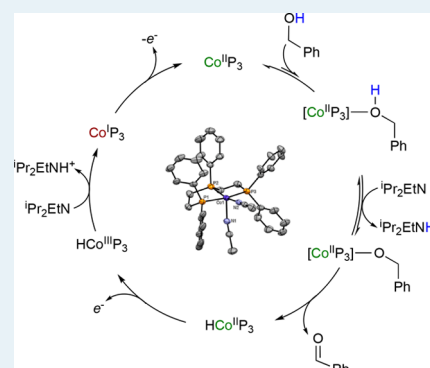
ACCESS |

Metrics & More

Article Recommendations

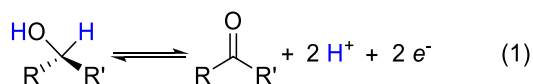
Supporting Information

**ABSTRACT:** Coordination of the tridentate ligand bis(2-diphenylphosphinoethyl)-phenylphosphine ( $P_3$ ) to cobalt forms  $[(CH_3CN)_2Co^{II}P_3](BF_4)_2$  ( $Co^{II}P_3$ ). In the presence of the Brønsted base  $^iPr_2EtN$ ,  $Co^{II}P_3$  electrocatalytically oxidizes benzyl alcohol (BnOH) to benzaldehyde at an applied potential of  $-630$  mV vs  $Fc^{+/0}$  with a TON of 19.9. In a noncatalytic reaction with excess BnOH and  $^iPr_2EtN$ ,  $Co^{II}P_3$  is reduced by one electron to  $[(CH_3CN)_2Co^IP_3]BF_4$  ( $Co^IP_3$ ) with concomitant formation of half an equivalent of benzaldehyde. This stoichiometric oxidation of BnOH suggests electron transfer occurs between intermediate cobalt species and starting  $Co^{II}P_3$ . Kinetics and computational studies support an unfavorable alcohol binding preequilibrium step followed by favorable deprotonation of the bound alcohol.



**KEYWORDS:** alcohol oxidation, catalysis, electrocatalysis, catalyst design, electrocatalyst, electrooxidation, cobalt

A major challenge for global energy markets is the efficient storage and use of energy from intermittent renewable sources. To address the needed scale, energy can be stored in the form of chemical bonds, such as those in alcohols. These fuels are attractive for energy storage because they are liquids and thereby offer high energy densities and safety advantages over gaseous fuels.<sup>1</sup> Efficient extraction of this energy necessitates development of electrocatalysts for oxidation of alcohols (eq 1).



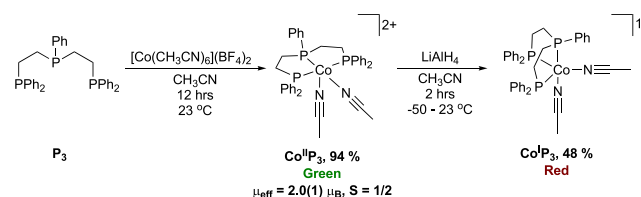
Despite a long history of molecular catalysts for alcohol oxidation,<sup>2–7</sup> the development of electrocatalysts for this transformation has been limited. Catalysts based on precious metals, including Ru,<sup>8–12</sup> Ir,<sup>13</sup> and Pd,<sup>14</sup> have been extensively studied. Only three catalysts derived from earth-abundant first-row transition metals (Fe,<sup>15</sup> Ni,<sup>16</sup> Cu<sup>17</sup>) have been reported. We seek to broaden the range of catalysts based on nonprecious metals by developing a novel electrocatalyst for the oxidation of alcohol as a critical step toward the utilization of renewable liquid fuels. In this pursuit, we have emphasized the synthetic tunability and the generation of acidic metal hydrides that can be deprotonated by alkyl amines.

Cobalt complexes have been used for alkylation reactions involving alcohol dehydrogenation<sup>18–21</sup> and the hydrogenation of aldehydes and ketones.<sup>22–24</sup> More importantly, Co–H complexes supported by phosphine donors are oxidized at mild

potentials to generate acidic protons,<sup>25,26</sup> making them candidates for electrocatalysis. We therefore targeted a cobalt complex of linear triphos,  $P_3$  ( $P_3$  = bis(2-diphenylphosphinoethyl)phenylphosphine) for electrocatalytic oxidation of alcohols, focusing in this work on benzyl alcohol as an initial target.

The complexes  $[(CH_3CN)_2Co^{II}P_3](BF_4)_2$  ( $Co^{II}P_3$ ) and  $[(CH_3CN)_2Co^IP_3]BF_4$  ( $Co^IP_3$ ) were synthesized according to Scheme 1. Both complexes were characterized by NMR spectroscopy, cyclic voltammetry (CV), X-ray diffraction, UV–vis spectroscopy, and elemental analysis. The crystal structures of  $Co^{II}P_3$  and  $Co^IP_3$  (Figure 1) reflect square-pyramidal ( $\tau_5$  =

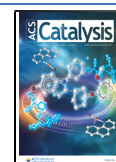
## Scheme 1. Synthesis of Triphos Cobalt Complexes



Received: February 18, 2021

Revised: April 18, 2021

Published: May 13, 2021



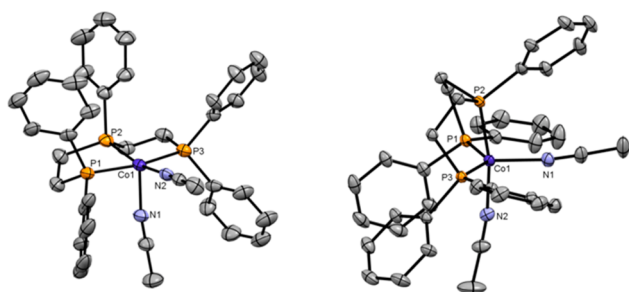


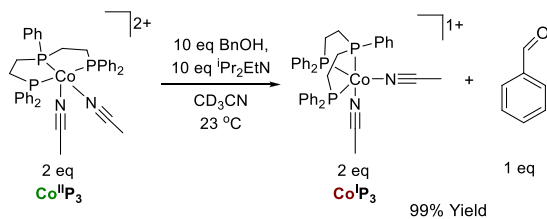
**Figure 1.** Crystal structures of  $\text{Co}^{\text{II}}\text{P}_3$  (left) and  $\text{Co}^{\text{I}}\text{P}_3$  (right). Hydrogen atoms and  $\text{BF}_4$  counterions are omitted for clarity.

0.03) and distorted trigonal-bipyramidal ( $\tau_5 = 0.9$ )<sup>27</sup> coordination environments, respectively. Metric parameters affiliated with both structures are normal compared with related Co complexes,<sup>25,28–31</sup> and detailed structural parameters are listed in the [Supporting Information](#).

CVs of  $\text{Co}^{\text{II}}\text{P}_3$  feature three redox couples (Figure S1). The cathodic reversible wave ( $E_{1/2} = -0.78$  V vs  $\text{Fc}^{+/0}$ ,  $\Delta E_p = 64$  mV) is assigned to the  $\text{Co}^{\text{II/I}}$  couple and is the feature expected to be relevant to electrocatalytic oxidation of alcohols. A second cathodic wave ( $E_{p/2} = -1.74$  V vs  $\text{Fc}^{+/0}$ ,  $\Delta E_p = 210$  mV) is assigned to the  $\text{Co}^{\text{I/0}}$  couple, and an anodic wave ( $E_{1/2} = +0.11$  V vs  $\text{Fc}^{+/0}$ ) is assigned to the  $\text{Co}^{\text{III/II}}$  couple. The second cathodic wave is irreversible, and the anodic wave has a large peak to peak separation of 308 mV, consistent with quasireversibility that likely results from solvent coordination that is coupled to electron transfer.<sup>32</sup> Additionally, the electrochemical behavior of  $\text{Co}^{\text{I}}\text{P}_3$  is consistent with that of the  $\text{Co}^{\text{II}}\text{P}_3$  complex (Figure S4).

Stoichiometric reactivity studies were undertaken with  $\text{Co}^{\text{II}}\text{P}_3$  to determine its efficacy as a catalyst for benzyl alcohol (BnOH) oxidation. Treating  $\text{Co}^{\text{II}}\text{P}_3$  and BnOH in acetonitrile- $d_3$  with  $^1\text{Pr}_2\text{EtN}$  immediately caused a color change from green to red (Scheme 2).  $^1\text{H}$  NMR spectroscopy confirmed nearly

### Scheme 2. Stoichiometric Oxidation of BnOH



quantitative formation of  $\text{Co}^{\text{I}}\text{P}_3$  and benzaldehyde in a 2:1 ratio. The reduction to  $\text{Co}^{\text{I}}$  is not surprising as alcohols have been used to reduce  $\text{Rh}^{\text{III}}$  and  $\text{Ir}^{\text{III}}$  complexes. Since oxidation of BnOH requires the loss of two electrons, the 2:1 product ratio suggests an electron transfer occurs from a second equivalent of  $\text{Co}^{\text{II}}\text{P}_3$  in solution. Treating  $\text{Co}^{\text{II}}\text{P}_3$  with BnOLi also produces  $\text{Co}^{\text{I}}\text{P}_3$  and benzaldehyde in a  $\sim$ 2:1 ratio (Scheme S1).

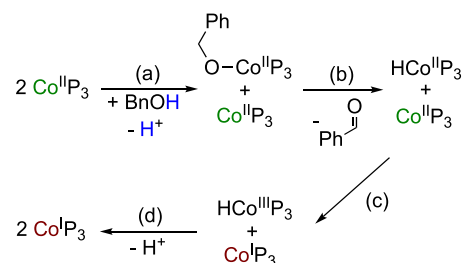
We propose that BnOH oxidation proceeds through a hydride complex  $[\text{HCoP}_3(\text{CH}_3\text{CN})_n]^+$  ( $\text{HCo}^{\text{II}}\text{P}_3$ ,  $n = 0-2$ ) that is formed by  $\beta$ -hydride elimination from an alkoxide ligand. This hydride complex is then susceptible to oxidation. Monomeric  $\text{Co}^{\text{II}}$  alkoxide complexes are known, but all lack  $\beta$ -hydrogens,<sup>35–39</sup> with only one exception.<sup>40</sup> While we were unable to isolate or directly observe  $\text{HCo}^{\text{II}}\text{P}_3$  because of rapid

conversion to  $\text{Co}^{\text{I}}\text{P}_3$ , isolable  $\text{Co}^{\text{II}}$  hydride complexes supported by pincer ligands have been reported<sup>41–43</sup> and are known to undergo one-electron reduction.  $\beta$ -Hydride elimination from Ir alkoxide complexes has been observed,<sup>44</sup> and supporting mechanistic studies on  $\beta$ -eliminations from  $\text{Rh}^{\text{III}}$ <sup>45</sup> and  $\text{Ir}^{\text{III}}$ <sup>44,46,47</sup> alkoxides are also known. Furthermore, isotopic labeling experiments for Co-catalyzed acceptorless dehydrogenations implicate hydride species formed through  $\beta$ -elimination.<sup>21</sup>

During the stoichiometric oxidation of BnOH, multiple reaction pathways are possible after the  $\beta$ -hydride elimination. First a net hydrogen atom transfer reaction between two equivalents of  $\text{HCo}^{\text{II}}\text{P}_3$  is possible, analogous to the reactivity of bis-diphosphine hydride complexes,  $[\text{HM}(\text{dppe})_2]^+$  ( $\text{M} = \text{Co},^{25} \text{Rh}, \text{Ir}^{48}$ ). This pathway should form  $\text{Co}^{\text{I}}\text{P}_3$  and the dihydride complex  $[(\text{H})_2\text{CoP}_3(\text{CH}_3\text{CN})_n]^+$  ( $(\text{H})_2\text{Co}^{\text{III}}\text{P}_3$ ,  $n = 0-1$ ), which is expected to be diamagnetic.<sup>26</sup> However, no hydridic resonances are observed in the  $^1\text{H}$  NMR spectrum of the reaction mixture. Alternatively, conversion of  $\text{HCo}^{\text{II}}\text{P}_3$  to  $\text{Co}^{\text{I}}\text{P}_3$  and  $1/2 \text{H}_2$  is possible.<sup>26,49</sup> However, gas chromatographic analysis of the reaction headspace revealed no detectible  $\text{H}_2$ . Most importantly, neither of these pathways provides the necessary 2:1 product ratio.

Scheme 3 illustrates the proposed explanation for the experimentally observed 2:1 ratio of  $\text{Co}^{\text{I}}\text{P}_3$  to aldehyde. In the

### Scheme 3. Proposed Pathway for the Stoichiometric Oxidation of BnOH



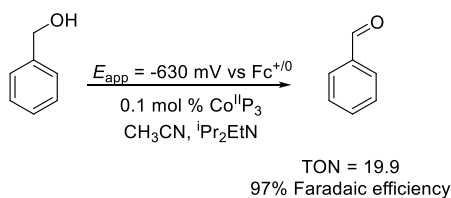
first step (Scheme 3a), one equivalent of  $\text{Co}^{\text{II}}\text{P}_3$  reacts with BnOH and base, generating an alkoxide species  $\text{BnOCo}^{\text{II}}\text{P}_3$  which proceeds to release the product aldehyde and a putative  $\text{HCo}^{\text{II}}\text{P}_3$  (Scheme 3b). Presumably, this process occurs through  $\beta$ -hydride elimination (vide supra).

Oxidation of  $\text{HCo}^{\text{II}}\text{P}_3$  by the parent complex  $\text{Co}^{\text{II}}\text{P}_3$  should be energetically favorable (Scheme 3c). Thermochemical data from Ciancanelli and co-workers showed that the (III/II) couple for the cationic complex  $[\text{HCo}(\text{dppe})_2]^+$  is 130 mV negative of the (II/I) couple of the parent  $[\text{Co}(\text{dppe})_2]^+$  complex.<sup>25</sup> Similar behavior is expected in the present system, suggesting that the cationic  $\text{HCo}^{\text{II}}\text{P}_3$  can undergo electron transfer with the parent  $\text{Co}^{\text{II}}\text{P}_3$ , generating  $\text{Co}^{\text{I}}\text{P}_3$  and  $\text{HCo}^{\text{III}}\text{P}_3$  (Scheme 3c). The latter species should be sufficiently acidic to be deprotonated by  $^1\text{Pr}_2\text{EtN}$ ,<sup>25,26</sup> forming a second equivalent of  $\text{Co}^{\text{I}}\text{P}_3$  (Scheme 3d).

To test for electrocatalytic activity, two types of experiments were performed. First, CV studies were performed in the presence of alcohol and base. A cathodically scanned CV of  $\text{Co}^{\text{II}}\text{P}_3$  in the presence of BnOH displayed the reversible  $\text{Co}^{\text{II/I}}$  couple (Figure S31).  $\text{Co}^{\text{I}}\text{P}_3$  was then generated *in situ* by addition of  $^1\text{Pr}_2\text{EtN}$ . Reduction to  $\text{Co}^{\text{I}}\text{P}_3$  was confirmed by an anodic scan across the  $\text{Co}^{\text{II/I}}$  couple. However, no current enhancement was observed under these conditions, suggesting

that the electrocatalysis is slower than the voltametric time scale, even at low scan rates (Figures S36–S37). Second, controlled-potential electrolysis was performed (Scheme 4).

#### Scheme 4. Electrocatalytic Oxidation of BnOH<sup>a</sup>



<sup>a</sup>[BnOH]<sub>0</sub> = 536 mM, [iPr<sub>2</sub>EtN]<sub>0</sub> = 619 mM, [Co<sup>II</sup>P<sub>3</sub>] = 0.51 mM, 2.25 h, T = 25 °C.

The applied potential ( $E_{\text{app}}$ ) for the electrolysis experiment was set to 150 mV positive of the observed Co<sup>II/I</sup> couple ( $E_{\text{app}} = -630$  mV vs Fc<sup>+/0</sup>). After 2.25 h, the current plateaued and a total charge of 105.1 C was passed yielding a turnover number (TON) of 19.9 (Figure S32). Quantitative <sup>1</sup>H NMR spectroscopy confirmed the production of benzaldehyde (TON = 19.3; 97% Faradaic efficiency) but did not show any resonances corresponding to Co<sup>I</sup>P<sub>3</sub>, suggesting catalyst decomposition during electrolysis. Correspondingly, CVs taken following the electrolysis revealed over a 90% loss in current of the Co<sup>II/I</sup> couple (Figure S33).

Kinetics studies using the chemical oxidant FeCp<sup>\*</sup><sub>2</sub>BF<sub>4</sub><sup>50</sup> were then undertaken to determine the factors influencing the rates of alcohol oxidation by Co<sup>II</sup>P<sub>3</sub>. NMR-scale experiments showed that Co<sup>II</sup>P<sub>3</sub> catalytically converts benzyl alcohol to benzaldehyde (TON = 8.8, See Supporting Information). Because of overlapping product and ligand <sup>1</sup>H resonances, 4-fluorobenzyl alcohol was chosen as a model substrate, and the rates of alcohol oxidation were determined using <sup>19</sup>F NMR spectroscopy.

Catalytic reactions were performed at 25 °C in CD<sub>3</sub>CN in the presence of varying amounts of alcohol, iPr<sub>2</sub>EtN, Co<sup>II</sup>P<sub>3</sub>, and FeCp<sup>\*</sup><sub>2</sub><sup>+</sup> (Table S2) under pseudo-first order conditions with FeCp<sup>\*</sup><sub>2</sub><sup>+</sup> as the limiting reagent (TON<sub>max</sub> = 5–10). A 3-fold increase in [FeCp<sup>\*</sup><sub>2</sub><sup>+</sup>]<sub>0</sub> (38–114 mM) led to a minor (1.3-fold) change in % conversion (58–75%, Figure S20), suggesting a zero-order dependence on [FeCp<sup>\*</sup><sub>2</sub><sup>+</sup>]<sub>0</sub>. Because the kinetic traces exhibit significant deviation from linearity (Figures S21–S23), the data could not be fit to obtain  $k_{\text{obs}}$  values. Instead, percent conversion to 4-fluorobenzaldehyde at 500 s was examined as a proxy for rate. Increasing [iPr<sub>2</sub>EtN]<sub>0</sub> and [Co<sup>II</sup>P<sub>3</sub>]<sub>0</sub> resulted in a linear increase in conversion to product after 500 s, indicating first-order dependencies on base and catalyst (Figures 2 and S20). Saturation behavior was observed for alcohol across the range of [Alcohol]<sub>0</sub> = 140–1140 mM (Figure 2), consistent with pre-equilibrium alcohol binding.

Several factors can potentially explain the nonideal behavior observed in the full kinetic traces and the nonzero intercepts in plots of percent conversion vs [iPr<sub>2</sub>EtN]<sub>0</sub> and [Co<sup>II</sup>P<sub>3</sub>]<sub>0</sub> (Figures 2 and S20). First, based on the stoichiometric reactivity studies described above, Co<sup>II</sup>P<sub>3</sub> can act as both a catalyst and an oxidant. In addition, alcohol coordination to Co, presumably accompanied by solvent dissociation, is necessary for iPr<sub>2</sub>EtN to deprotonate benzyl alcohol (O–H pK<sub>a</sub>(CH<sub>3</sub>CN) ~ 28).<sup>51</sup> In acetonitrile, the rate laws for both associative and dissociative ligand substitution most likely

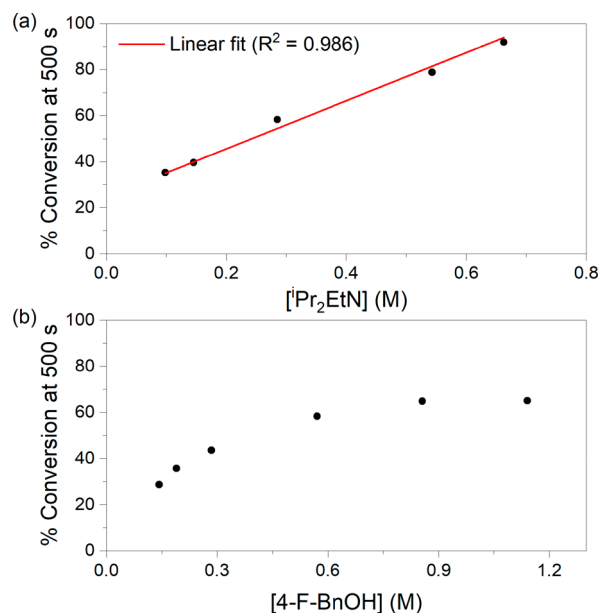


**Figure 2.** Percent conversion of 4-fluorobenzyl alcohol to 4-fluorobenzaldehyde in the presence of Co<sup>II</sup>P<sub>3</sub> and FeCp<sup>\*</sup><sub>2</sub><sup>+</sup> at 500 s as a function of base (a) and alcohol (b) concentration. Percent conversion is calculated as [Aldehyde]<sub>500 s</sub>/[Aldehyde]<sub>max</sub> where [Aldehyde]<sub>max</sub> = 1/2 [FeCp<sup>\*</sup><sub>2</sub><sup>+</sup>]<sub>0</sub> + [Co<sup>II</sup>P<sub>3</sub>]<sub>0</sub>. Further details are provided in the Supporting Information.

contain solvent-dependent terms, possibly leading to nonzero intercepts in percent conversion versus [substrate]<sub>0</sub> plots.<sup>52–54</sup> Furthermore, <sup>1</sup>H NMR spectroscopic analyses of the reaction mixture indicate catalyst decomposition over time, and UV–vis experiments show that Co<sup>II</sup>P<sub>3</sub> slowly decomposes in the presence of iPr<sub>2</sub>EtN (Figures S17–S18). Despite these complications, the kinetics studies are consistent with pre-equilibrium binding of alcohol and deprotonation occurring in the rate-limiting transition state or in a pre-equilibrium process.

DFT calculations were performed to gain insight into the thermodynamic landscape of the reaction. Note that barriers were not calculated, and therefore the calculations do not identify kinetically favored reaction pathways but rather provide information about the structures and relative free energies of potential intermediates. Figure 3 illustrates the calculated free-energy profile for the oxidation of BnOH to benzaldehyde. Ligand substitution by BnOH is thermodynamically unfavorable by +9.4 and +13.5 kcal/mol for axial (1'-HOBN<sub>ax</sub>) and equatorial (1'-HOBN<sub>eq</sub>) isomers, respectively, which is consistent with the lack of observed alcohol adducts and the saturation behavior. Calculations suggest that deprotonation of bound BnOH by iPr<sub>2</sub>EtN is favorable, leading to the alkoxides 2'-OBN<sub>ax</sub> and 2'-OBN<sub>eq</sub> via reactions that are exergonic by –1.0 and –9.7 kcal/mol, respectively.

Calculations suggest CH<sub>3</sub>CN loss forming 3'-OBN<sub>eq</sub> prior to 4'-H<sub>ax</sub>. Generation of an intermediate 16e<sup>-</sup> complex (3'-OBN<sub>eq</sub>) is expected for a β-elimination process, but a concerted process cannot be ruled out. The optimized geometry of the lowest free energy hydride species 4'-H<sub>ax</sub> reveals a bent P<sub>3</sub> ligand (∠P1–Co–P3 = 157°), relieving the steric interaction of the apical η<sup>1</sup>-aldehyde and lowering the energy of the d<sub>x<sup>2</sup>-y<sup>2</sup></sub> σ\* orbital that accepts the hydride ligand.

From 4'-H<sub>ax</sub> exchange of PhCHO for CH<sub>3</sub>CN is favorable by more than 10 kcal/mol, leading to Co<sup>II</sup> hydride, 5'-H. The

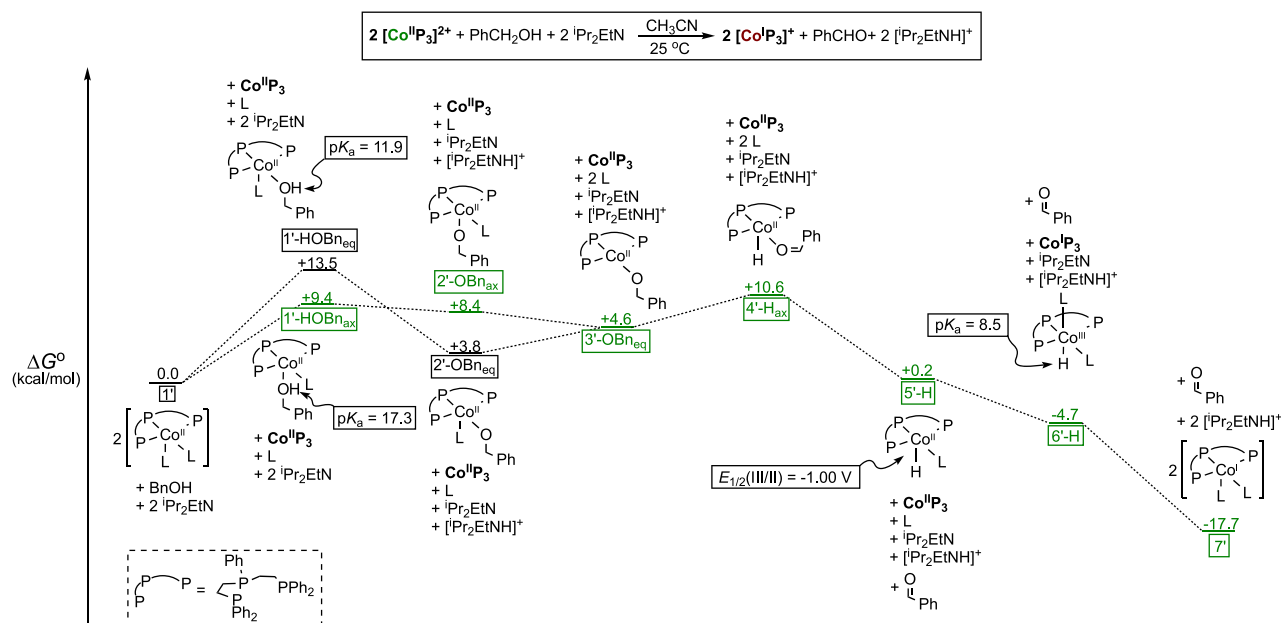


**Figure 3.** Computed free energies (in kcal/mol) for BnOH oxidation. Primes indicate calculated states; L = CH<sub>3</sub>CN; pK<sub>a</sub> values are given as absolute values assuming that the pK<sub>a</sub> value for the [iPr<sub>2</sub>EtNH]<sup>+</sup> is equal to that of [Et<sub>3</sub>NH]<sup>+</sup>; E<sub>1/2</sub> values are reported versus Fc<sup>+/0</sup> (E<sub>1/2</sub> = 0 V) by assigning the experimental potential for the Co<sup>II/I</sup> couple (−0.781 V versus Fc<sup>+/0</sup>). The DFT calculations were computed at the BP86/6-31G\*\* level with the LANL2DZ pseudopotential for cobalt and the SMD solvation model.<sup>51,52</sup> See the Supporting Information for details.

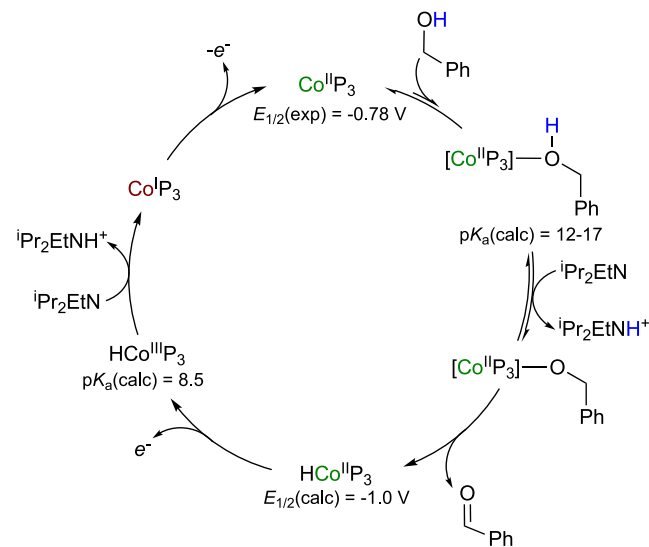
potential required to oxidize 5'-H to 6'-H is −1.00 V vs Fc<sup>+/0</sup> and includes solvent association to generate an acidic hydride (pK<sub>a</sub>(calc) = 8.5). The pK<sub>a</sub> of 5'-H was calculated to be 18.8, further supporting the mechanism of oxidation followed by deprotonation. The computed oxidation potential and pK<sub>a</sub> of 5'-H are in excellent agreement with experimental studies by Ciancanelli and are consistent with our reactivity studies showing that an electron transfer occurs between an intermediate hydride species and starting Co<sup>II</sup>P<sub>3</sub> (Scheme 3). Deprotonation leading to 7' (Co<sup>I</sup>P<sub>3</sub>) provides the thermodynamic impetus (ΔG° = −17.5 kcal/mol for 5'-H to 7') that drives BnOH oxidation. Overall, the calculations are consistent with the experimental observations of unfavorable alcohol binding, reactivity with alkyl amine base, and electron transfer from intermediate(s) such as 5'-H.

Scheme 5 illustrates a proposed catalytic cycle for BnOH oxidation based upon the kinetic and theoretical studies presented herein. The first step involves coordination of BnOH to Co<sup>II</sup>P<sub>3</sub>. The saturation kinetics, lack of an observable alcohol adduct, and computational results all suggest alcohol binding is unfavorable. Deprotonation of coordinated alcohol generates an alkoxide complex. This reaction sequence is supported by computations, the first-order dependence on base, and the reactivity of Co<sup>II</sup>P<sub>3</sub> with BnOLi. Calculations suggest the bound alkoxide can undergo β-hydride elimination, producing aldehyde and HCo<sup>III</sup>P<sub>3</sub>.

HCo<sup>III</sup>P<sub>3</sub> represents the point of divergence for the stoichiometric and catalytic pathways. Under catalytic conditions HCo<sup>III</sup>P<sub>3</sub> is oxidized by [FeCp\*<sub>2</sub>]<sup>+</sup> or the electrode; under stoichiometric conditions electron transfer between an equivalent of Co<sup>II</sup>P<sub>3</sub> and HCo<sup>III</sup>P<sub>3</sub> can occur. In both scenarios, an acidic HCo<sup>III</sup>P<sub>3</sub> complex is produced that can be readily deprotonated yielding Co<sup>I</sup>P<sub>3</sub>. Lastly, the cycle is closed by oxidation of Co<sup>I</sup>P<sub>3</sub> to Co<sup>II</sup>P<sub>3</sub>.

In summary, the Co<sup>II</sup>P<sub>3</sub> complex is capable of oxidizing BnOH under chemical and electrochemical conditions.

### Scheme 5. Proposed Catalytic Cycle for BnOH Oxidation



Controlled potential electrolysis experiments demonstrate that Co<sup>II</sup>P<sub>3</sub> electrocatalytically oxidizes benzyl alcohol with a TON = 19.9 at an applied potential of −630 mV vs Fc<sup>+/0</sup>. Stoichiometric reactivity studies indicate that electron transfer between Co<sup>II</sup>P<sub>3</sub> and an intermediate cobalt species leads to a 2:1 ratio of Co<sup>I</sup>P<sub>3</sub> to aldehyde. Kinetics studies suggest the reaction is first order in iPr<sub>2</sub>EtN and Co<sup>II</sup>P<sub>3</sub> and saturates in alcohol, consistent with an unfavorable alcohol binding pre-equilibrium.

To our knowledge, Co<sup>II</sup>P<sub>3</sub> is the first reported molecular electrocatalyst based on cobalt for the oxidation of alcohols. Although its TOF is lower than those of other first-row transition metal complexes, the number of catalytic turnovers observed under bulk electrolysis conditions is higher (20 turnovers compared with 2–3 for Fe(PNP)(CO)(H) and

Ni(P<sub>2</sub>N<sub>2</sub>)(L<sub>n</sub>)<sup>2+</sup>).<sup>15,16</sup> Since the thermodynamic potentials for oxidation of alcohols are not known in organic solvents, it is difficult to rigorously evaluate overpotentials. However, the overpotentials of Co<sup>II</sup>P<sub>3</sub> and Ni(P<sub>2</sub>N<sub>2</sub>)(L<sub>n</sub>)<sup>2+</sup> should be approximately equivalent based on their similar catalytic potentials and the use of trialkylamine bases in both systems.<sup>16</sup> In contrast, catalysis occurs ~400 mV more positive using Cu(bpy)/TEMPO,<sup>17</sup> and a much stronger base (phospha-zene) is required for Fe(PNP)(CO)(H),<sup>15</sup> resulting in higher driving forces and thereby overpotentials for both of these systems. Our present studies demonstrate the feasibility of developing new electrocatalysts for alcohol oxidation based on first-row transition metals, with opportunities for improving catalyst performance.

## ■ ASSOCIATED CONTENT

### Supporting Information

The Supporting Information is available free of charge at <https://pubs.acs.org/doi/10.1021/acscatal.1c00781>.

Synthetic and experimental procedures, characterization of new compounds, details of X-ray crystal structures, kinetic data and analysis, additional electrochemical data, and computational details and methods (PDF)  
Crystallographic data for [(CH<sub>3</sub>CN)<sub>2</sub>CoP<sub>3</sub>](BF<sub>4</sub>)<sub>2</sub> (CIF)  
Crystallographic data for [(CH<sub>3</sub>CN)<sub>2</sub>CoP<sub>3</sub>]BF<sub>4</sub> (CIF)

## ■ AUTHOR INFORMATION

### Corresponding Authors

**Aaron M. Appel** – Center for Molecular Electrocatalysis, Pacific Northwest National Laboratory, Richland, Washington 99352, United States; [orcid.org/0000-0002-5604-1253](https://orcid.org/0000-0002-5604-1253); Email: [aaron.appel@pnnl.gov](mailto:aaron.appel@pnnl.gov)

**Sharon Hammes-Schiffer** – Department of Chemistry, Yale University, New Haven, Connecticut 06520, United States; [orcid.org/0000-0002-3782-6995](https://orcid.org/0000-0002-3782-6995); Email: [sharon.hammes-schiffer@yale.edu](mailto:sharon.hammes-schiffer@yale.edu)

### Authors

**Spencer P. Heins** – Center for Molecular Electrocatalysis, Pacific Northwest National Laboratory, Richland, Washington 99352, United States

**Patrick E. Schneider** – Department of Chemistry, Yale University, New Haven, Connecticut 06520, United States

**Amy L. Speelman** – Center for Molecular Electrocatalysis, Pacific Northwest National Laboratory, Richland, Washington 99352, United States

Complete contact information is available at: <https://pubs.acs.org/doi/10.1021/acscatal.1c00781>

### Notes

The authors declare no competing financial interest.

## ■ ACKNOWLEDGMENTS

S.P.H. acknowledges Dr. Peter Dunn, Dr. Morris Bullock and Dr. Eric Wiedner for helpful discussions. This work was supported as part of the Center for Molecular Electrocatalysis, an Energy Frontier Research Center funded by the U.S. Department of Energy, Office of Science, Basic Energy Sciences. P.E.S. is also supported by a National Science Foundation Graduate Research Fellowship Grant No. DGE-1752134.

## ■ REFERENCES

- (1) Pearson, R. J.; Eisaman, M. D.; Turner, J. W. G.; Edwards, P. P.; Jiang, Z.; Kuznetsov, V. L.; Littau, K. A.; Di Marco, L.; Taylor, S. R. G. Energy Storage via Carbon-Neutral Fuels Made from CO<sub>2</sub>, Water, and Renewable Energy. *Proc. IEEE* **2012**, *100*, 440–460.
- (2) Meerwein, H.; Schmidt, R. New Method for the Reduction of Aldehydes and Ketones. *Liebigs Ann. Chem.* **1925**, *444*, 221–238.
- (3) Verley, A. The Exchange of Functional Groups between Two Molecules. The Passage of Ketones to Alcohols and the Reverse. *Bull. Soc. Chim. Fr.* **1925**, *37*, 871–874.
- (4) Ponndorf, W. Der Reversible Austausch Der Oxydationsstufen Zwischen Aldehyden Oder Ketonen Einerseits Und Primären Oder Sekundären Alkoholen Andererseits. *Angew. Chem.* **1926**, *39*, 138–143.
- (5) Oppenauer, R. V. Dehydration of Secondary Alcohols to Ketones. I. Preparation of Sterol Ketones and Sex Hormones. *Recl. Trav. Chim. Pays-Bas* **1937**, *56*, 137–144.
- (6) Schultz, M. J.; Sigman, M. S. Recent Advances in Homogeneous Transition Metal-Catalyzed Aerobic Alcohol Oxidations. *Tetrahedron* **2006**, *62*, 8227–8241.
- (7) Conley, B. L.; Pennington-Boggio, M. K.; Boz, E.; Williams, T. J. Discovery, Applications, and Catalytic Mechanisms of Shvo's Catalyst. *Chem. Rev.* **2010**, *110*, 2294–2312.
- (8) Catalano, V. J.; Heck, R. A.; Immoos, C. E.; Öhman, A.; Hill, M. G. Steric Modulation of Electrocatalytic Benzyl Alcohol Oxidation by [Ru(Trpy)(R<sub>2</sub>dppi)(O)]<sup>2+</sup> Complexes. *Inorg. Chem.* **1998**, *37*, 2150–2157.
- (9) Liu, Y. P.; Zhao, S. F.; Guo, S. X.; Bond, A. M.; Zhang, J.; Zhu, G.; Hill, C. L.; Geletii, Y. V. Electrooxidation of Ethanol and Methanol Using the Molecular Catalyst [{Ru<sub>4</sub>O<sub>4</sub>(OH)<sub>2</sub>(H<sub>2</sub>O)<sub>4</sub>}(γ-SiW<sub>10</sub>O<sub>36</sub>)<sub>2</sub>]<sup>10-</sup>. *J. Am. Chem. Soc.* **2016**, *138*, 2617–2628.
- (10) Moyer, B. A.; Thompson, M. S.; Meyer, T. J. Chemically Catalyzed Net Electrochemical Oxidation of Alcohols, Aldehydes, and Unsaturated Hydrocarbons Using the System (Trpy)(Bpy)Ru(OH<sub>2</sub>)<sup>2+</sup>/(Trpy)(Bpy)RuO<sup>2+</sup>. *J. Am. Chem. Soc.* **1980**, *102*, 2310–2312.
- (11) Rodríguez, M.; Romero, I.; Llobet, A.; Deronzier, A.; Biner, M.; Parella, T.; Stoeckli-Evans, H. Synthesis, Structure, and Redox and Catalytic Properties of a New Family of Ruthenium Complexes Containing the Tridentate Bpea Ligand. *Inorg. Chem.* **2001**, *40*, 4150–4156.
- (12) Waldie, K. M.; Flajlslik, K. R.; McLoughlin, E.; Chidsey, C. E. D.; Waymouth, R. M. Electrocatalytic Alcohol Oxidation with Ruthenium Transfer Hydrogenation Catalysts. *J. Am. Chem. Soc.* **2017**, *139*, 738–748.
- (13) Bonitatibus, P. J.; Rainka, M. P.; Peters, A. J.; Simone, D. L.; Doherty, M. D. Highly Selective Electrocatalytic Dehydrogenation at Low Applied Potential Catalyzed by an Ir Organometallic Complex. *Chem. Commun.* **2013**, *49*, 10581–10583.
- (14) Serra, D.; Correia, M. C.; McElwee-White, L. Iron and Ruthenium Heterobimetallic Carbonyl Complexes as Electrocatalysts for Alcohol Oxidation: Electrochemical and Mechanistic Studies. *Organometallics* **2011**, *30*, 5568–5577.
- (15) McLoughlin, E. A.; Matson, B. D.; Sarangi, R.; Waymouth, R. M. Electrocatalytic Alcohol Oxidation with Iron-Based Acceptorless Alcohol Dehydrogenation Catalyst. *Inorg. Chem.* **2020**, *59*, 1453–1460.
- (16) Weiss, C. J.; Wiedner, E. S.; Roberts, J. A. S.; Appel, A. M. Nickel Phosphine Catalysts with Pendant Amines for Electrocatalytic Oxidation of Alcohols. *Chem. Commun.* **2015**, *51*, 6172–6174.
- (17) Badalyan, A.; Stahl, S. S. Cooperative Electrocatalytic Alcohol Oxidation with Electron-Proton-Transfer Mediators. *Nature* **2016**, *535*, 406–410.
- (18) Deibl, N.; Kempe, R. General and Mild Cobalt-Catalyzed C-Alkylation of Unactivated Amides and Esters with Alcohols. *J. Am. Chem. Soc.* **2016**, *138*, 10786–10789.
- (19) Rösler, S.; Ertl, M.; Irrgang, T.; Kempe, R. Cobalt-Catalyzed Alkylation of Aromatic Amines by Alcohols. *Angew. Chem., Int. Ed.* **2015**, *54*, 15046–15050.

- (20) Daw, P.; Chakraborty, S.; Garg, J. A.; Ben-David, Y.; Milstein, D. Direct Synthesis of Pyrroles by Dehydrogenative Coupling of Diols and Amines Catalyzed by Cobalt Pincer Complexes. *Angew. Chem., Int. Ed.* **2016**, *55*, 14373–14377.
- (21) Zhang, G.; Hanson, S. K. Cobalt-Catalyzed Acceptorless Alcohol Dehydrogenation: Synthesis of Imines from Alcohols and Amines. *Org. Lett.* **2013**, *15*, 650–653.
- (22) Zhang, G.; Scott, B. L.; Hanson, S. K. Mild and Homogeneous Cobalt-Catalyzed Hydrogenation of C = C, C = O, and C = N Bonds. *Angew. Chem., Int. Ed.* **2012**, *51*, 12102–12106.
- (23) Xu, R.; Chakraborty, S.; Yuan, H.; Jones, W. D. Acceptorless, Reversible Dehydrogenation and Hydrogenation of N-Heterocycles with a Cobalt Pincer Catalyst. *ACS Catal.* **2015**, *5*, 6350–6354.
- (24) Zhang, G.; Vasudevan, K. V.; Scott, B. L.; Hanson, S. K. Understanding the Mechanisms of Cobalt-Catalyzed Hydrogenation and Dehydrogenation Reactions. *J. Am. Chem. Soc.* **2013**, *135*, 8668–8681.
- (25) Ciancanelli, R.; Noll, B. C.; DuBois, D. L.; DuBois, M. R. Comprehensive Thermodynamic Characterization of the Metal-Hydrogen Bond in a Series of Cobalt-Hydride Complexes. *J. Am. Chem. Soc.* **2002**, *124*, 2984–2992.
- (26) Marinescu, S. C.; Winkler, J. R.; Gray, H. B. Molecular Mechanisms of Cobalt-Catalyzed Hydrogen Evolution. *Proc. Natl. Acad. Sci. U. S. A.* **2012**, *109*, 15127–15131.
- (27) Addison, A. W.; Rao, T. N.; Reedijk, J.; van Rijn, J.; Verschoor, G. C. Synthesis, Structure, and Spectroscopic Properties of Copper(II) Compounds Containing Nitrogen–Sulphur Donor Ligands; the Crystal and Molecular Structure of Aqua[1,7-Bis(N-Methylbenzimidazol-2'yl)-2,6-Dithiaheptane]Copper(II) Perchlorate. *J. Chem. Soc., Dalton Trans.* **1984**, 1349–1356.
- (28) Jiang, F.; Wei, G.; Huang, Z.; Lei, X.; Hong, M.; Kang, B.; Liu, H. Syntheses and Crystal Structures of Two Thiolato-Organophosphino Cobalt(II) Complexes,  $(Et_4N)[Co(SC_6H_5)_2(PPh_3)]$  and  $[Co(S-m-C_6H_4CH_3)_2(Ph_2PCH_2CH_2P(Ph)CH_2CH_2PPh_2)]$ . *J. Coord. Chem.* **1992**, *25*, 183–191.
- (29) Mason, R.; Scollary, G. R. The Crystal Structure of Two Cobalt(I) Complexes Containing the Polyphosphine Ligands  $PhP\{(CH_2)NPPH_2\}_2$  ( $n = 2, 3$ ). *Aust. J. Chem.* **1977**, *30*, 2395–2406.
- (30) Wei, G.; Hong, M.; Huang, Z.; Liu, H. Stereochemistry of Mixed Thiolate and Diteriary Phosphine Cobalt(II) Complexes. Crystal Structures of  $[Co\{Ph_2P(CH_2)_3PPh_2\}(SPh)_2]$  and  $[Co\{Ph_2PCH_2CH_2P(Ph)CH_2CH_2PPh_2\}(SPh)_2]$ . *J. Chem. Soc., Dalton Trans.* **1991**, 3145–3148.
- (31) Chen, J. F.; Li, C. Enol Ester Synthesis via Cobalt-Catalyzed Regio- and Stereoselective Addition of Carboxylic Acids to Alkynes. *Org. Lett.* **2018**, *20*, 6719–6724.
- (32) Böttcher, A.; Takeuchi, T.; Hardcastle, K. I.; Meade, T. J.; Gray, H. B.; Cwikel, D.; Kapon, M.; Dori, Z. Spectroscopy and Electrochemistry of Cobalt(III) Schiff Base Complexes. *Inorg. Chem.* **1997**, *36*, 2498–2504.
- (33) Giordano, G.; Crabtree, R. H.; Heintz, R. M.; Forster, D.; Morris, D. E. Di- $\mu$ -Chloro-Bis( $\eta^1$ -1,5-Cyclooctadiene)-Dirhodium(I). *Inorg. Synth.* **1990**, *28*, 88–90.
- (34) Van Der Ent, A.; Onderdelinden, A. L.; Schunn, R. A. Chlorobis(Cyclooctene)Rhodium(I) and-Iridium(I) Complexes. *Inorg. Synth.* **1990**, *28*, 90–92.
- (35) Jayasundara, C. R. K.; Sabasovs, D.; Staples, R. J.; Oppenheimer, J.; Smith, M. R.; Maleczka, R. E. Cobalt-Catalyzed C-H Borylation of Alkyl Arenes and Heteroarenes Including the First Selective Borylations of Secondary Benzylic C-H Bonds. *Organometallics* **2018**, *37*, 1567–1574.
- (36) Bellow, J. A.; Stoian, S. A.; Van Tol, J.; Ozarowski, A.; Lord, R. L.; Groysman, S. Synthesis and Characterization of a Stable High-Valent Cobalt Carbene Complex. *J. Am. Chem. Soc.* **2016**, *138*, 5531–5534.
- (37) Bellow, J. A.; Yousif, M.; Fang, D.; Kratz, E. G.; Cisneros, G. A.; Groysman, S. Synthesis and Reactions of 3d Metal Complexes with the Bulky Alkoxide Ligand  $[OC^tBu_2Ph]$ . *Inorg. Chem.* **2015**, *54*, 5624–5633.
- (38) Olmstead, M. M.; Power, P. P.; Sigel, G. Mononuclear Cobalt(II) Complexes Having Alkoxide and Amide Ligands: Synthesis and X-Ray Crystal Structures of  $[Co(Cl)(OC-tert-Bu_3)_2Li(THF)_3]$ ,  $[Li(THF)_{4.5}[Co\{N(SiMe_3)_2\}(OC-tert-Bu_3)_2]$ , and  $[Li\{Co(N(SiMe_3)_2)(OC-tert-Bu_3)_2\}]$ . *Inorg. Chem.* **1986**, *25*, 1027–1033.
- (39) Bryndza, H. E.; Tam, W. Monomeric Metal Hydroxides, Alkoxides, and Amides of the Late Transition Metals: Synthesis, Reactions, and Thermochemistry. *Chem. Rev.* **1988**, *88*, 1163–1188.
- (40) Tubbs, K. J.; Szajna, E.; Bennett, B.; Halfen, J. A.; Watkins, R. W.; Arif, A. M.; Berreau, L. M. Mononuclear Nitrogen/Sulfur-Ligated Cobalt (II) Methoxide Complexes: Structural, EPR, Paramagnetic  $^1H$  NMR, and Electrochemical Investigations. *Dalton Trans.* **2004**, 2398–2399.
- (41) Kuriyama, S.; Arashiba, K.; Tanaka, H.; Matsuo, Y.; Nakajima, K.; Yoshizawa, K.; Nishibayashi, Y. Direct Transformation of Molecular Dinitrogen into Ammonia Catalyzed by Cobalt Dinitrogen Complexes Bearing Anionic PNP Pincer Ligands. *Angew. Chem., Int. Ed.* **2016**, *55*, 14291–14295.
- (42) Wu, S.; Li, X.; Xiong, Z.; Xu, W.; Lu, Y.; Sun, H. Synthesis and Reactivity of Silyl Iron, Cobalt, and Nickel Complexes Bearing a [PSiP]-Pincer Ligand via Si–H Bond Activation. *Organometallics* **2013**, *32*, 3227–3237.
- (43) Merz, L. S.; Blasius, C. K.; Wadepohl, H.; Gade, L. H. Square Planar Cobalt(II) Hydride versus T-Shaped Cobalt(I): Structural Characterization and Dihydrogen Activation with PNP–Cobalt Pincer Complexes. *Inorg. Chem.* **2019**, *58*, 6102–6113.
- (44) Blum, O.; Milstein, D. Mechanism of a Directly Observed. Beta-Hydride Elimination Process of Iridium Alkoxo Complexes. *J. Am. Chem. Soc.* **1995**, *117*, 4582–4594.
- (45) Pàmies, O.; Bäckvall, J. Studies on the Mechanism of Metal-Catalyzed Hydrogen Transfer from Alcohols to Ketones. *Chem. - Eur. J.* **2001**, *7*, 5052–5058.
- (46) Ritter, J. C. M.; Bergman, R. G. A Useful Method for Preparing Iridium Alkoxides and a Study of Their Catalytic Decomposition by Iridium Cations: A New Mode of  $\beta$ -Hydride Elimination for Coordinatively Saturated Metal Alkoxides. *J. Am. Chem. Soc.* **1998**, *120*, 6826–6827.
- (47) Zhao, J.; Hesslink, H.; Hartwig, J. F. Mechanism of  $\beta$ -Hydrogen Elimination from Square Planar Iridium(I) Alkoxide Complexes with Labile Dative Ligands. *J. Am. Chem. Soc.* **2001**, *123*, 7220–7227.
- (48) Pilloni, G.; Schiavon, G.; Zotti, G.; Zecchin, S. Electrochemistry of Coordination Compounds XV. Paramagnetic Hydrido Complexes of Cobalt(II), Rhodium(II) and Iridium(II). *J. Organomet. Chem.* **1977**, *134*, 305–318.
- (49) Monfette, S.; Turner, Z. R.; Semproni, S. P.; Chirik, P. J. Enantioselective C 1-Symmetric Bis(Imino)Pyridine Cobalt Complexes for Asymmetric Alkene Hydrogenation. *J. Am. Chem. Soc.* **2012**, *134*, 4561–4564.
- (50) Weiss, C. J.; Das, P.; Miller, D. L.; Helm, M. L.; Appel, A. M. Catalytic Oxidation of Alcohol via Nickel Phosphine Complexes with Pendant Amines. *ACS Catal.* **2014**, *4*, 2951–2958.
- (51) Ugur, I.; Marion, A.; Parant, S.; Jensen, J. H.; Monard, G. Rationalization of the  $pK_a$  Values of Alcohols and Thiols Using Atomic Charge Descriptors and Its Application to the Prediction of Amino Acid  $pK_a$ 's. *J. Chem. Inf. Model.* **2014**, *54*, 2200–2213.
- (52) Cheeseman, T. P.; Odell, A. L.; Raethel, H. A. Trans-Effect Order for Alkene, Alkyne, Phosphine, Arsine, Stibine, and Sulphide Ligands from Studies of Diethylamine Exchange Reactions of  $L_2PtCl_2$ ,  $[^{14}C]NH_2$ , in Various Solvents. *Chem. Commun.* **1968**, 1496–1498.
- (53) Richens, D. T. Ligand Substitution Reactions at Inorganic Centers. *Chem. Rev.* **2005**, *105*, 1961–2002.
- (54) Langford, C. H.; Gray, H. B. *Ligand Substitution Processes*; W. A. Benjamin, Inc.: New York, 1966.